JOURNAL OF PROPULSION AND POWER
Vol. 20, No. 3, May–June 2004

Full- and Partial-Admission Performance of the Simplex Turbine

Daniel J. Dorney* and Lisa W. Griffin†
NASA Marshall Space Flight Center, Huntsville, Alabama 35812
Douglas L. Sondak‡
Boston University, Boston, Massachusetts 02215

The turbines used in rocket-engine applications are often partial-admission turbines, meaning that the flow enters the rotor over only a portion of the annulus. These turbines have been traditionally analyzed, however, assuming full-admission characteristics. This assumption enables the simulation of only a portion of the 360-deg annulus with periodic boundary conditions applied in the circumferential direction. Whereas this traditional approach to simulating the flow in partial-admission turbines significantly reduces the computational requirements, the accuracy of the solutions has not been evaluated or compared to partial-admission data. In the current investigation, both full-admission and partial-admission three-dimensional unsteady Navier–Stokes simulations were performed for a partial-admission turbine designed and tested at NASA Marshall Space Flight Center. The results indicate that the partial-admission nature of the turbine should be included in simulations to properly predict the performance and flow unsteadiness of the turbine.

Nomenclature

C = axial chord
M = Mach number
P = static pressure
P_t = total pressure
T_t = total temperature
X = axial distance
W = work
α = absolute circumferential angle
β = relative circumferential angle
η = total-to-total efficiency

Introduction

PARTIAL-ADMISSION turbines are used in many high-speed, low-flow applications, especially in rocket engines. In a partial-admission environment the flow enters the turbine rotor over only a portion of the complete annulus. Thus, the turbine rotors periodically pass through flowing regions and regions of no flow. The turbine airfoils, therefore, operate in an unsteady flow environment that is strongly dependent on the circumferential location of the airfoils. Historically, partial-admission turbines have been analyzed using full-admission flow assumptions, namely, that the flow is periodic and that only a portion of the annulus need be simulated. The impact of this assumption on the design and predicted performance of partial-admission turbines has not been thoroughly investigated. While there is little in the literature discussing numerical simulations of partial-admission flows, theoretical and experimental studies of partial-admission turbines include the works of Stenning,[1] Horlock,[2] Boulbin et al.,[3] and Huzel and Huang.[4] These four references contain empirical correlations for designing partial-admission turbines and estimating their performance.

Received 5 August 2002; accepted for publication 12 May 2003.

*Aerospace Engineer, Applied Fluid Dynamics Analysis Group, TD 64. Associate Fellow AIAA.
†Team Leader, Applied Fluid Dynamics Analysis Group, TD 64. Senior Member AIAA.
‡Senior Scientific Programmer, Office of Information Technology, III Cummington Street. Senior Member AIAA.

The objective of the current study is to characterize the unsteady and time-averaged flowfields in a partial-admission turbine by performing full- and partial-admission simulations of the Simplex turbine. This study will help to assess the inaccuracies due to the full-admission assumption commonly used for design purposes. The Simplex turbopump was designed to support the ground testing of a hybrid propulsion system. This system utilizes a gas-generator cycle resulting in a low-flow, partial-admission supersonic turbine. Computational simulations of the Simplex turbine were performed using a three-dimensional time-dependent Navier–Stokes analysis. The numerical results were compared with limited experimental data and exhibited reasonable agreement.

Numerical Procedure

The governing equations considered in this study are time-dependent, three-dimensional Reynolds-averaged Navier–Stokes equations. The algorithm consists of a time-marching, implicit, finite difference scheme. The procedure is third-order spatially accurate and second-order temporally accurate. The inviscid fluxes are discretized according to the scheme developed by Roe.[5] The viscous fluxes are calculated using standard central differences. An approximate-factorization technique is used to compute the time rate changes in the primary variables. Newton subiterations are used at each global time step to increase stability and reduce linearization errors. For all cases investigated in this study, one Newton subiteration was performed at each time step. Additional Newton iterations were not necessary because a small time step was chosen to resolve all the expected frequencies of interest. The turbulent viscosity is calculated using the two-layer Baldwin–Lomax algebraic turbulence model.[6] Message-passing interface and OpenMP application program interfaces are used for parallel processing to reduce the computation time.

The Navier–Stokes analysis uses O- and H-type zonal grids to discretize the flowfield and facilitate relative motion of the rotating components (see Fig. 1). The O grids are body-fitted to the surfaces of the airfoils and generated using an elliptic equation solution procedure. They are used to properly resolve the viscous flow in the blade passages and to easily apply the algebraic turbulence model. The algebraically generated H grids are used to discretize the remainder of the flowfield, including the nozzles.

The computational analysis was validated on several supersonic turbine geometries.[7–10]

Geometry and Flow Conditions

The single-stage supersonic turbine, called Simplex, includes straight centerline nozzles and was designed and tested as a

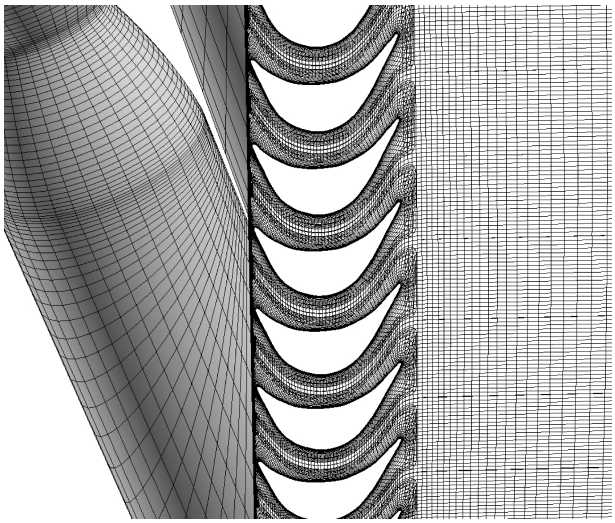

Fig. 1 Computational grids for the nozzles and rotors.

turbopump component at NASA Marshall Space Flight Center. The turbine was tested with both metallic and composite rotor airfoils, and the time-averaged static temperatures and total pressures were recorded at three circumferential locations at the turbine exit. Two of the circumferential locations were in flowing regions, whereas one was in a nonflowing region. The experimental total-to-total efficiency was determined using measured static quantities and derived total quantities and by numerically averaging results at the three circumferential locations. Further details of the Simplex experiments can be found in Ref. 11.

The boundary conditions for the numerical simulations were based on the design flow conditions. The flow enters the nozzles at the design total pressure of $P_t = 801$ psia (55.2 MPa), a total temperature of 799 R (444 K) and in the axial direction ($\alpha = 0.0$ deg). The design total-to-static pressure ratio across the complete turbine is $P_{\text{exit}}/P_{t-\text{inlet}} = 15.67$. The operating fluid in the rig tests was gaseous nitrogen, whereas the operating fluid in the engine and current simulations is gaseous oxygen. Oxygen was used in the simulations to support the goals of the engine project.

The Simplex turbine geometry includes 6 straight centerline nozzles, flowing over half the annulus, and 95 rotors. In the full-admission simulation it was assumed that the turbine contained 12 nozzles (i.e., equally spaced flowing nozzles around the annulus) and 96 rotors, with the rotors being scaled by the factor of 95/96. A one-nozzle/eight-rotor model was then simulated. In the partial-admission simulation the actual turbine geometry of 6 flowing nozzles (covering half the annulus) and 95 rotors was simulated. The spanwise sectional grids for the rotors in both simulations contained approximately 5000 grid points. The grid density for the spanwise sections was determined by performing two-dimensional simulations. The full-admission simulations utilized 31 spanwise planes, while the partial-admission simulations utilized 15 spanwise planes. The number of spanwise planes in the full-admission simulation was based on previous work,[7,8] whereas the use of 15 spanwise planes in the partial-admission simulation was deemed acceptable based on the length scales of the unsteadiness associated with the nozzles. Each straight centerline nozzle was modeled with approximately 270,000 grid points. Thus, a total of approximately 1.3 million grid points were used in the full-admission simulation and approximately 7.1 million grid points were used in the partial-admission simulation. The computational grids for the nozzles and rotors are shown in Fig. 1, where every other grid point has been removed for clarity.

Both simulations were run for almost 1.5 rotor revolutions. The time periodicity of the solution was verified by interrogating pressure traces at various locations in the nozzles and on the rotor blades. The simulations were performed on 17 to 38 450-MHz processors of an SGI Origin2000 located at NASA Ames Research Center. The simulations required approximately 3×10^{-6} s per grid point per iteration of CPU time per processor on 38 processors.

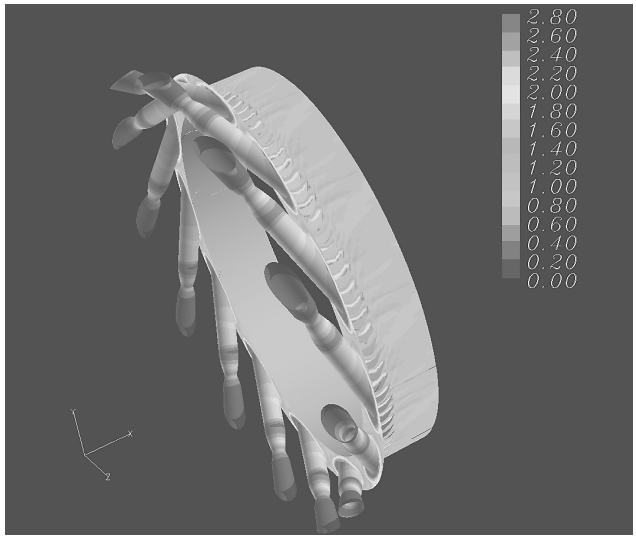

Fig. 2 Instantaneous Mach contours: upstream view, full admission.

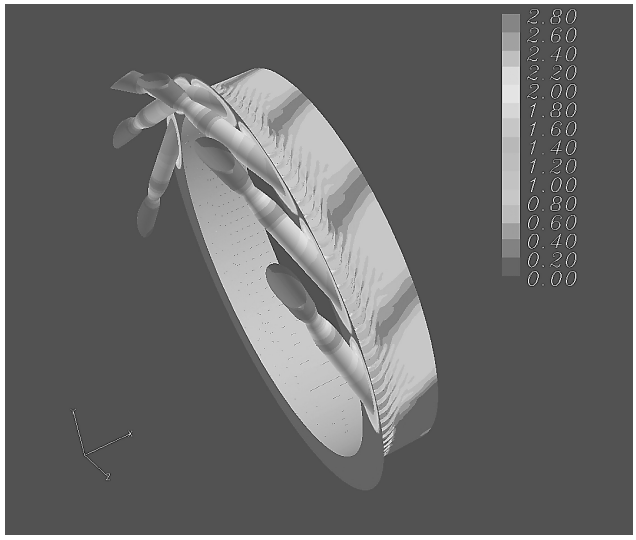

Fig. 3 Instantaneous Mach contours: upstream view, partial admission.

Results

Instantaneous absolute Mach contours for the entire turbine (nozzles and rotors) in the full-admission and partial-admission simulations are shown in Figs. 2 and 3, respectively. In the partial-admission simulation the thick wakes associated with the solid-wall regions between adjacent nozzles are clearly visible. The low-speed flow regions outside the influence of the nozzles are also evident near the bottom of Fig. 3. In the full-admission simulation there is a subsonic flow region at the nozzle exit that causes a higher static pressure entering the rotor. Therefore, there is a greater acceleration in the rotor to achieve the prescribed exit pressure. The relative Mach number in the full-admission simulation remains supersonic to the turbine exit.

Tables 1 and 2 contain the mass- and time-averaged flow quantities at the inlet and exit of the nozzles and rotors, respectively. Note that in Table 1 the total pressure, total temperature, and flow angle are specified, whereas the mass flow, Mach number, and static pressure are derived as part of the solution process. In Table 2 the static pressure at the rotor exit is specified using the design pressure ratio, whereas all other flow quantities are derived.

The flow quantities at the nozzle inlet (see Table 1) are similar, except that the mass flow in the full-admission simulation is twice that of the partial-admission simulation. The average Mach number and total pressure are higher at the nozzle exit in the partial-admission

Table 1 Nozzle inlet and exit flow quantities

	Inlet		Exit	
Variable	Full admission	Partial admission	Full admission	Partial admission
M	0.274	0.254	1.06	1.39
α, deg	0	0	−73.4	−74.1
P, psia	75.4	76.1	78.9	78.6
P_t, psia	801	801	316	434
T_t, R	799	799	789	786
Flow, lbm/s	16.6	8.3	16.6	8.3

Table 2 Rotor inlet and exit flow quantities

	Inlet		Exit	
Variable	Full admission	Partial admission	Full admission	Partial admission
M, abs	0.925	0.874	0.664	0.410
M, rel	0.612	0.737	1.183	0.769
α, deg	−56.7	−68.5	28.2	2.70
β, deg	−22.8	26.8	61.2	71.1
P, psia	114.0	72.8	51.1	51.1
P_t, abs psia	280	208	70.5	61.8
P_t, rel psia	157	116	126	89.6
T_t, abs R	767	757	540	585
T_t, rel R	681	710	639	652
Flow, lbm/s	16.6	8.3	16.6	8.3
η_{t-t}	——	——	63.3	50.4
W, Btu/lbm	——	——	57.3	44.0

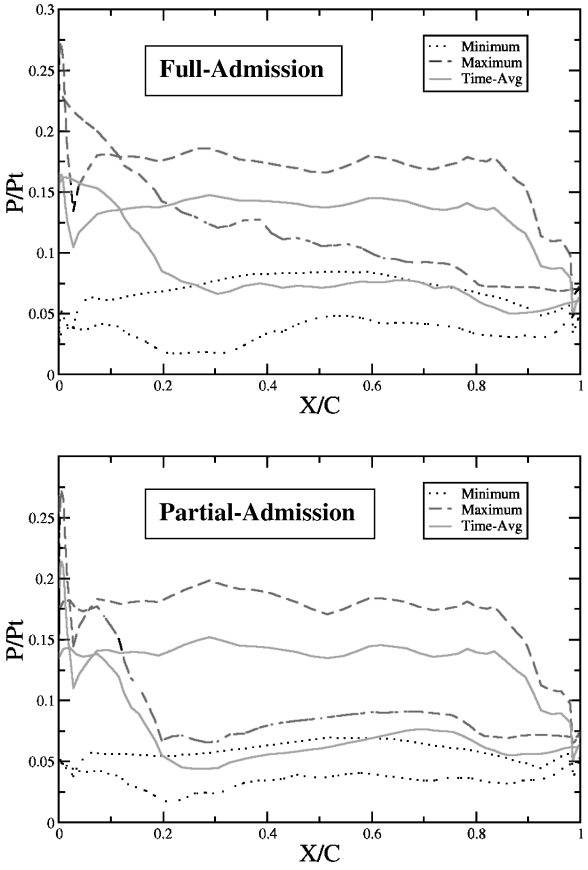

Fig. 4 Rotor midspan unsteady pressure envelops.

simulation. As noted earlier, the differences are caused by the rotor exerting a strong backpressure effect in the full-admission simulation. The large differences in the rotor inlet and exit conditions (see Table 2) are the result of including the region of low flow outside the influence of the flowing nozzles in the averaging process for the partial-admission simulation. Confining the averaging process to the regions of the annulus influenced by the flowing nozzles results in closer agreement of the flow quantities but disregards the important partial-admission flow phenomena. The efficiency and work in the full-admission simulation are, as expected, greater than in the partial-admission simulation. In the experiments the determination of the efficiency was based in part on three probes located at different circumferential locations at the exit of the rotor. Two of the probes were located within the influence of the flowing nozzles, while one was in the low-flow region. Thus, the experimental efficiency of $\eta = 60.5\%$ should be biased toward the value predicted in the full-admission simulation. Indeed, the experimental efficiency is bracketed by the predicted partial-admission value of $\eta = 50.4\%$ and full-admission value of $\eta = 63.3\%$. The discrepancies between the experimental and predicted efficiencies are likely the result of many sources: 1) the tests were run in nitrogen and the simulations were run for oxygen (engine conditions), 2) there were limitations of the computational grid density, and 3) there was a small number of data-acquisition locations used in the experiments.

Figure 4 displays unsteady pressure envelopes at midpsan from the full- and partial-admission simulations. Both simulations exhibit relatively constant loading across the span, whereas the full-admission simulation indicates significantly more unsteadiness. It is worth noting that the rotor does not become completely unloaded as it moves through the region outside of the flowing nozzles.

Unsteady pressure traces at various locations along the midspan of the rotor are shown for the full- and partial-admission simulations in Figs. 5 and 6, respectively. Figures 7 and 8 contain the Fourier decompositions corresponding to the pressure traces in Figs. 5 and 6. In the full-admission simulation the dominant unsteadiness on the suction surface is the nozzle-passing frequency (approximately 5000 Hz), while the pressure surface and trailing-edge regions experience significant unsteadiness at both the fundamental and twice the nozzle-passing frequency. The harmonic content is generated by two sources: 1) the pressure variations across the nozzle exit, and 2) the reflection of the rotor bow shock off the solid region between adjacent nozzles. The dominant unsteadiness when the rotors are in the nozzle jets in the partial-admission simulation is at the nozzle-passing frequency, although a moderate amount of unsteadiness is also present at twice the nozzle-passing frequency. As expected, when the rotor traverses both flowing and nonflowing regions in the partial-admission simulation the higher harmonic content (especially that associated with rotor bow shock reflection) is reduced and more low-frequency content is observed. It is interesting to note

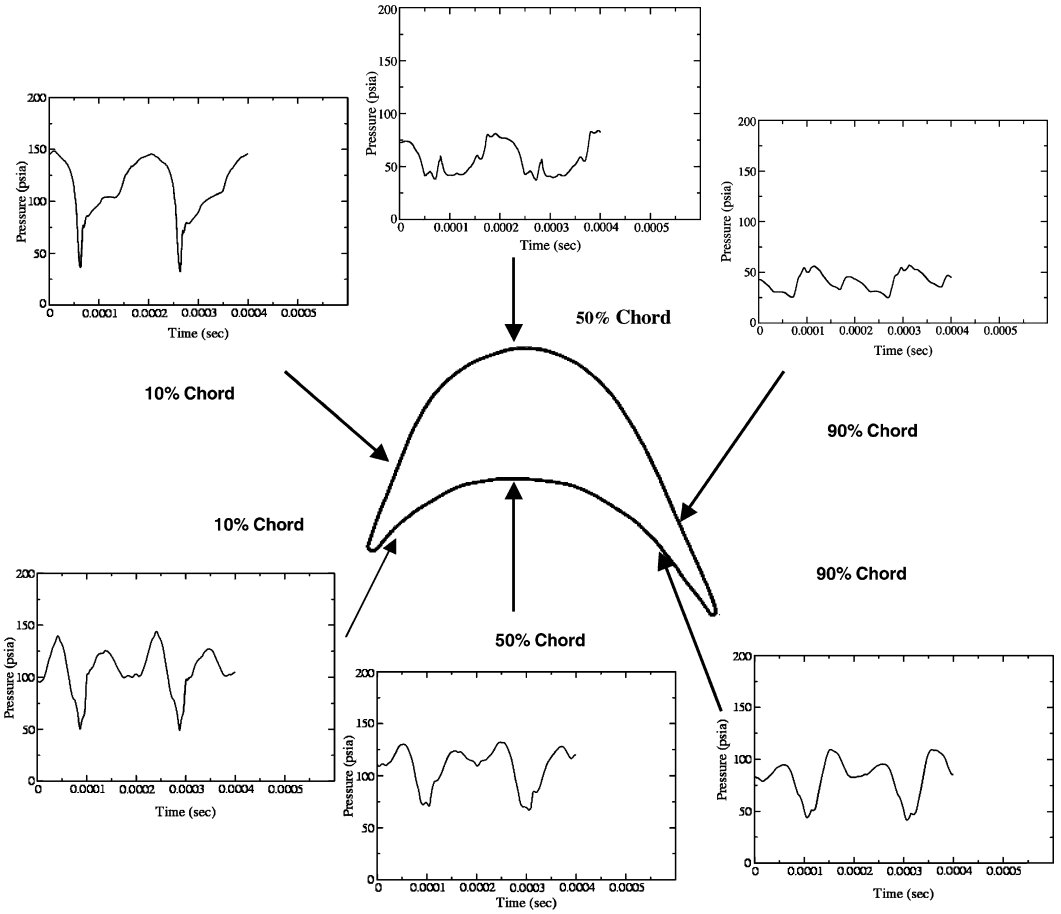

Fig. 5 Unsteady pressure traces: full admission, 50% span.

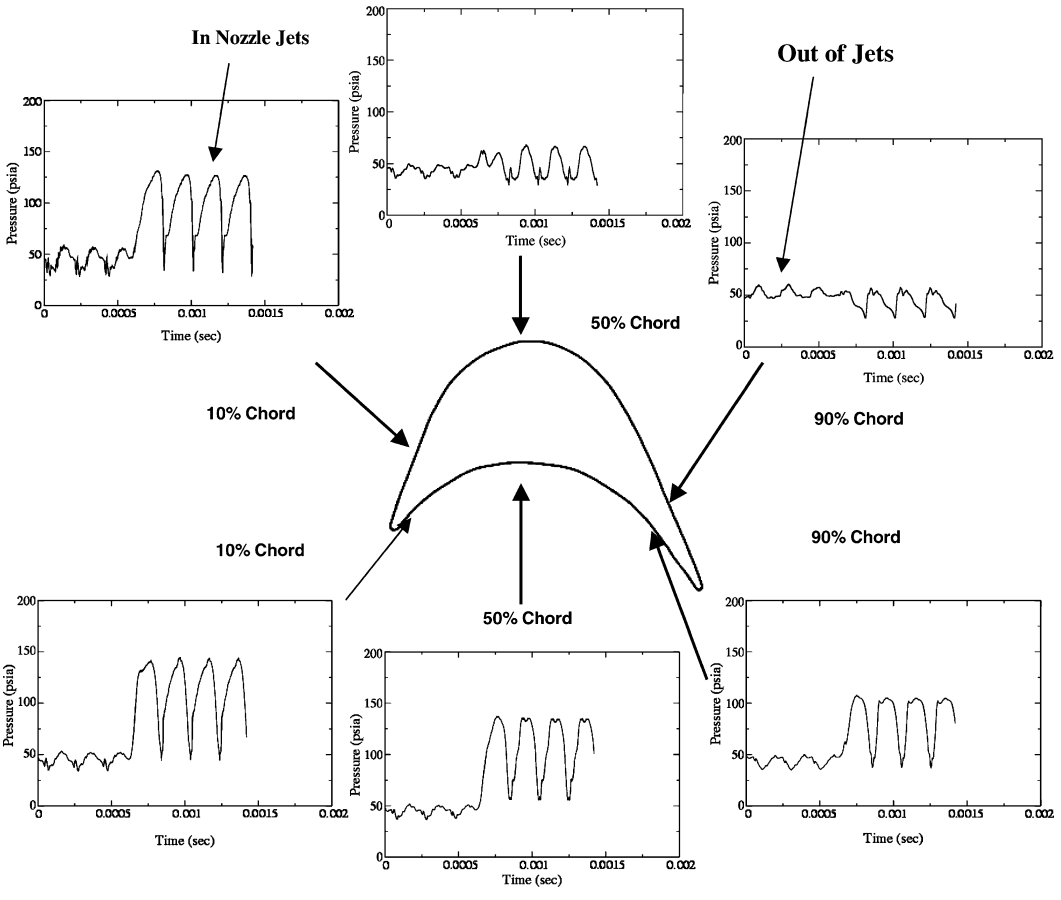

Fig. 6 Unsteady pressure traces: partial-admission, 50% span.

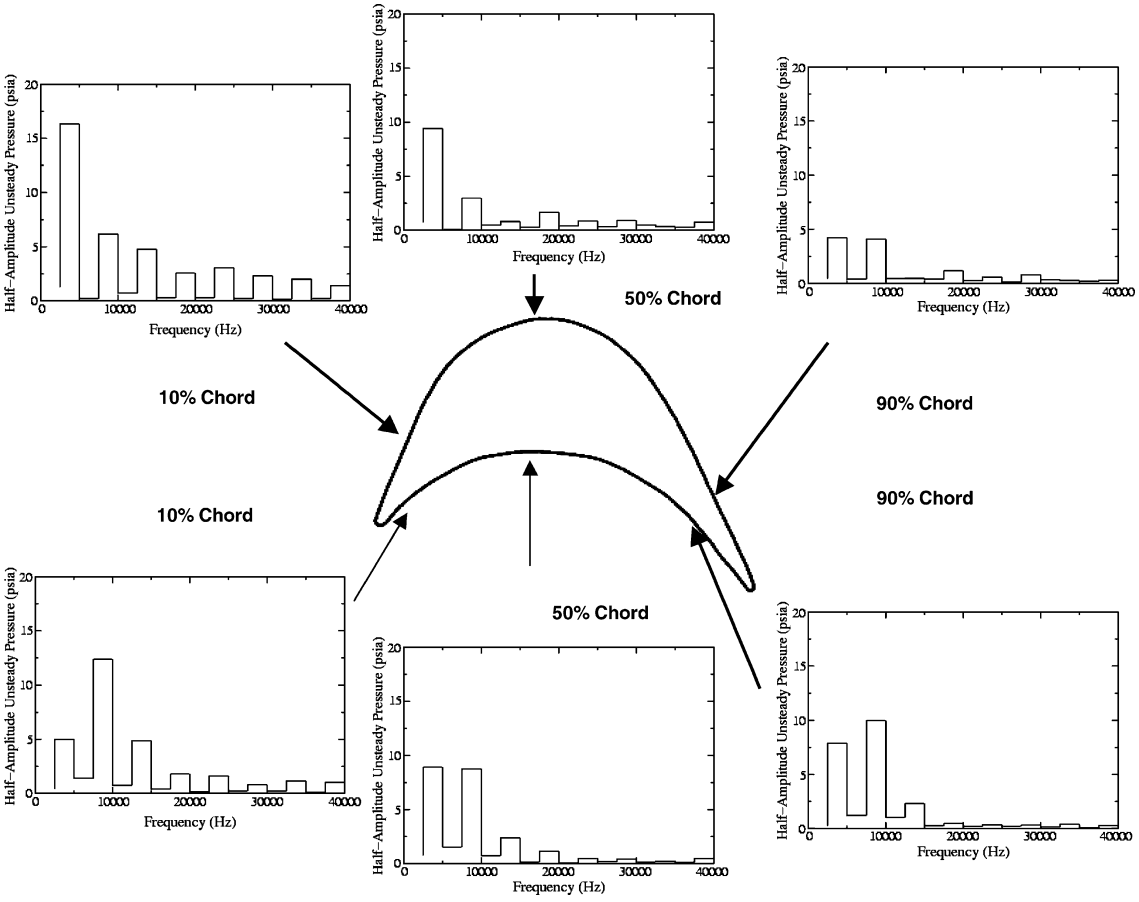

Fig. 7 Decomposition of unsteady pressure: full-admission, 50% span.

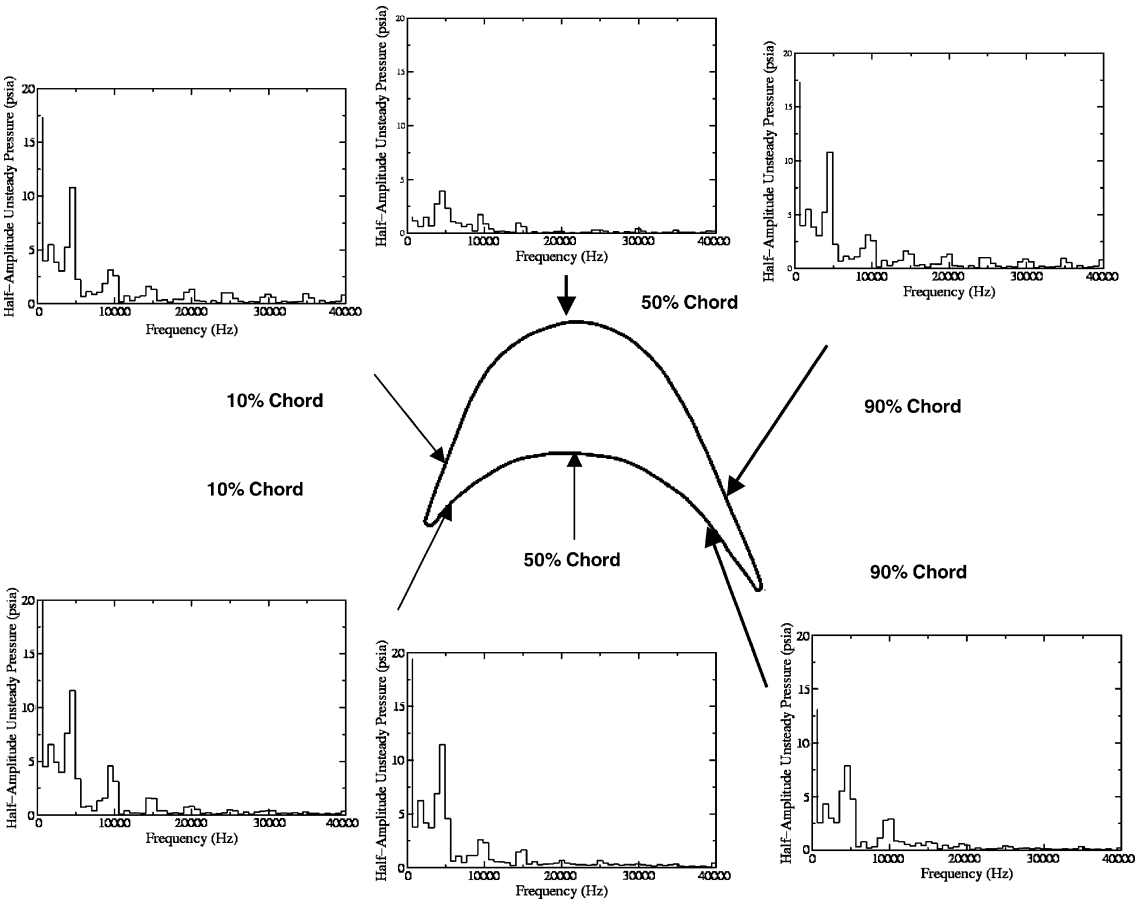

Fig. 8 Decomposition of unsteady pressure: partial-admission, 50% span.

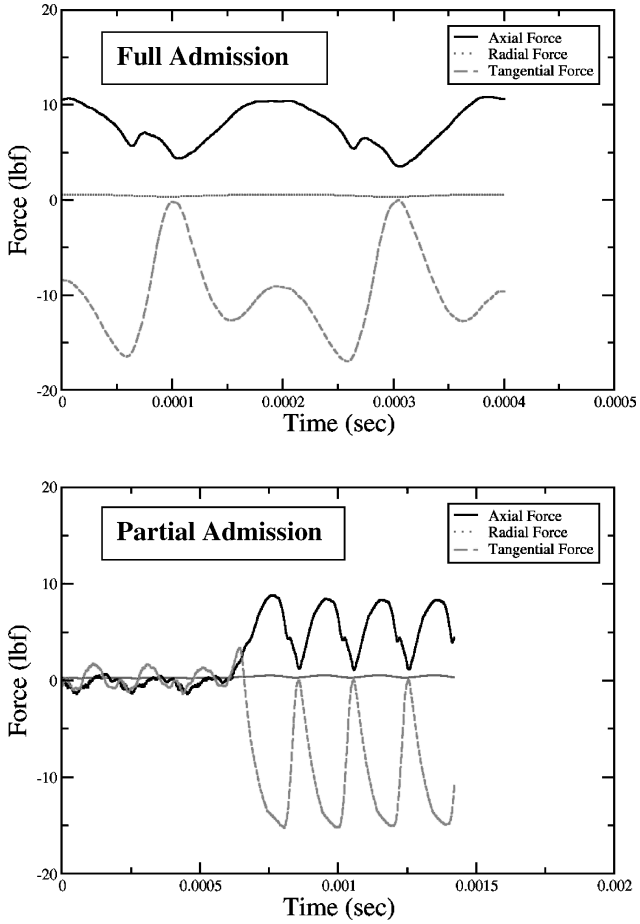

Fig. 9 Unsteady forces.

that even when the rotors are outside the flowing nozzle regions they still experience unsteadiness associated with the nozzle-passing frequency, albeit at a lower level. This implies that the interactions between the rotors and nozzles drive the unsteadiness of the entire system, not just the flowing portion of the annulus.

The unsteady axial, radial, and tangential forces on the rotors from the two simulations are shown in Fig. 9. The overall levels of the forces are similar in both simulations. The forces in the full-admission simulation exhibit two peaks as the rotors move through the nozzle flow. These peaks are generated by the presence of the subsonic flow over a portion of the nozzle exit. As expected, the results of the partial-admission simulation indicate that the rotors windmill when outside the region of the flowing nozzles.

Conclusions

Full- and partial-admission unsteady three-dimensional simulations were performed for a partial-admission supersonic turbine designed and tested at NASA Marshall Space Flight Center. The results of the partial-admission simulation show favorable agreement with the design Mach numbers and velocity triangles in the nozzles and rotors. The results of the full-admission simulation exhibit fair agreement with the experimental efficiency, which was determined by probes biased toward the flowing regions of the annulus. The full- and partial-admissions simulations gave significantly different nozzle-exit flow profiles and rotor velocity fields. The partial-admission rotor exit relative Mach number is subsonic, which is the design intent. In the full-admission simulation, however, the relative Mach number remains supersonic to the rotor exit. The differences between the results of the two simulations underscore the need for more computational and experimental studies of partial-admission geometries. Partial-admission simulations, such as the one described in this paper, are currently being used in the design of several new supersonic turbines.

References

[1]Stenning, A. H., "Design of Turbines for High-Energy-Fuel Low-Power-Output Applications," Massachusetts Inst. of Technology, Dynamic Analysis and Control Lab., Rept. 79, Sept. 1953.

[2]Horlock, J. H., *Axial Flow Turbines*, Butterworths, London, 1966, Chap. 7.

[3]Boulbin, F., Penneron, N., Kermarec, J., and Pluviose, M., "Turbine Blade Forces Due to Partial Admission," *Revue Francaise de Mecanique*, 1992–1993.

[4]Huzel, D. K., and Huang, D. H., *Design of Liquid-Propellant Rocket Engines*, Progress in Astronautics and Aeronautics, edited by A. R. Seebass, Vol. 147, AIAA, Washington, DC, 1992, Chap. 6.

[5]Roe, P. L., "Approximate Riemann Solvers, Parameter Vectors, and Difference Schemes," *Journal of Computational Physics*, Vol. 43, 1981, pp. 357–372.

[6]Baldwin, B. S., and Lomax, H., "Thin Layer Approximation and Algebraic Model for Separated Turbulent Flow," AIAA Paper 78-257, Jan. 1978.

[7]Griffin, L. W., and Dorney, D. J., "Simulations of the Unsteady Flow Through the Fastrac Supersonic Turbine," *Journal of Turbomachinery*, Vol. 122, No. 2, 2000, pp. 225–233.

[8]Dorney, D. J., Griffin, L. W., and Huber, F., "A Study of the Effects of Tip Clearance in a Supersonic Turbine," *Journal of Turbomachinery*, Vol. 122, No. 4, 2000, pp. 674–673.

[9]Dorney, D. J., Griffin, L. W., Huber, F., and Sondak, D. L., "Unsteady Flow in a Supersonic Turbine Stage with Variable Specific Heats," *Journal of Propulsion and Power*, Vol. 18, No. 2, 2002, pp. 493–496.

[10]Papila, N., Shyy, W., Griffin, L. W., and Dorney, D. J., "Shape Optimization of Supersonic Turbines Using Response Surface and Neural Network Methods," *Journal of Propulsion and Power*, Vol. 18, No. 3, 2002, pp. 509–518.

[11]Scallhorn, P. A., Majumdar, A., Van Hooser, K., and Marsh, M., "Flow Simulation in Secondary Flow Passages of a Rocket Engine Turbopump," AIAA Paper 98-3684, 1998.